IOP PUBLISHING FLUID *DYNAMICS* RESEARCH

Fluid Dyn. Res. **41** (2009) 000000 (21pp) doi:10.1088/0169-5983/41/1/000000

CICLoPE—a response to the need for high Reynolds number experiments

Alessandro Talamelli[1], Franco Persiani[1], Jens H M Fransson[2,6], P Henrik Alfredsson[2], Arne V Johansson[2], Hassan M Nagib[3], Jean-Daniel Rüedi[4], Katepalli R Sreenivasan[4] and Peter A Monkewitz[5]

[1] II Facoltà di Ingegneria, Università di Bologna, I-47100 Forlí, Italy
[2] Linné FLOW Centre, KTH Mechanics, Royal Institute of Technology, S-100 44 Stockholm, Sweden
[3] IIT, Chicago, IL 60616, USA
[4] ICTP, I-34014 Trieste, Italy
[5] Fluid Mechanics Laboratory, EPFL, 1015 Lausanne, Switzerland

E-mail: xxx Q1

Received 1 June 2007, in final form xx Q2
Published xx January 2009
Online at stacks.iop.org/FDR/41/000000

Communicated by Y Tsuji

Abstract

Although the equations governing turbulent flow of fluids are well known, understanding the overwhelming richness of flow phenomena, especially in high Reynolds number turbulent flows, remains one of the grand challenges in physics and engineering. High Reynolds number turbulence is ubiquitous in aerospace engineering, ground transportation systems, flow machinery, energy production (from gas turbines to wind and water turbines), as well as in nature, e.g. various processes occurring in the planetary boundary layer. High Reynolds number turbulence is not easily obtained in the laboratory, since in order to have good spatial resolution for measurements, the size of the facility itself has to be large. In this paper, we discuss limitations of various existing facilities and propose a new facility that will allow good spatial resolution even at high Reynolds number. The work is carried out in the framework of the Center for International Cooperation in Long Pipe Experiments (CICLoPE), an international collaboration that many in the turbulence community have shown an interest to participate in.

[6] Part of this paper was presented by JHMF at the 'Workshop on High Reynolds Experiments', 10 September, 2006, Nagoya, Japan.

0169-5983/09/000000+21$30.00

1. Introduction

The possibility to probe and understand turbulence dynamics, in general, has taken a giant leap with the increase of computing power. However, even with the world's largest computers, Reynolds numbers attainable remain moderate in fully resolved direct numerical simulations (DNS) of turbulent flows, and are not likely to reach the higher values of practical interest for decades to come. Also, the computational time needed to obtain good statistical significance at high Reynolds numbers of even the mean flow quantities is excessive, and for higher moments and spectra the required convergence time is prohibitive.

High Reynolds numbers are critically important in order to draw conclusions regarding the general nature of turbulence flow physics, the practical engineering situations in aeronautics, naval applications and energy conversion processes, as well as in many geophysical situations. Turbulence dynamics at high Reynolds numbers are important in neutral and stratified atmospheric boundary layers, in associated processes of importance for mixing and dilution of pollutants, and in aspects of climate modeling. The determination of the form of the mean velocity distribution in the overlap region is also a first step in the study of interaction between the large, essentially inviscid, outer scales and the viscously influenced, highly anisotropic, near-wall structures. DNS have recently advanced to the point where we start to see a real-scale separation between inner and outer scales, and new findings are emerging on the role of their interaction. The former becomes increasingly dominant with the increasing Reynolds number, and although DNS is giving us valuable information, there are a number of outstanding questions in turbulence research that can only be answered by studying turbulence at high Reynolds numbers under well-controlled conditions.

The definition of the Reynolds number

$$Re = \frac{\rho U L}{\mu}$$

reveals that various possibilities exist to obtain high Re; i.e. the velocity (U) may be increased (but not to such high levels that compressibility effects come into play), the density (ρ) can be elevated (for instance, by pressurizing a gas flow facility), or the physical dimensions (L) could be made large. In addition to a high Reynolds number, it is necessary to have a facility where the spatial size of the smallest scales is sufficiently large to be resolvable by available measurement techniques. A measure of the smallest scale is the viscous length scale ($\ell_* = \nu/u_\tau$, where ν is the kinematic viscosity and u_τ the friction velocity), and it can easily be shown that for a pipe-flow experiment with radius R, the following relation holds:

$$\ell_* = \frac{R}{Re_\tau}, \tag{1}$$

where $Re_\tau = u_\tau R/\nu$ and Re_τ is nearly proportional to Re. Therefore, it is clear that in order to have large scales at high Re, the overall dimension of the facility should be as large as possible.

The Center for International Cooperation in Long Pipe Experiments (CICLoPE[7]) is an initiative to establish a laboratory, where large-scale facilities can be installed, thereby, readily allowing the high-resolution turbulent fluctuations and detailed flow-structure measurements. It will also become the ideal laboratory to develop new, and further enhance current measurement techniques for turbulent flows. An existing excavated tunnel complex inside a hill in the town of Predappio, Italy, has been chosen for its location near the campus of the second faculty of engineering of the University of Bologna, and will ensure a stable

[7] www.ciclope.unibo.it

environment and small ambient disturbances. The laboratory belongs to the University of Bologna but its operation will be the concerns of the international consortium CICLoPE.

In the present paper, we are discussing a number of issues related to high Reynolds number experiments in turbulence. In section 2, we try to establish criteria for what can be considered a 'good' high Reynolds number experiment of wall-bounded turbulence. Section 3 reviews recent experiments in pipe, channel and boundary layer flows, whereas section 4 outlines some research issues suitable for a high Reynolds number facility. The design features of the proposed CICLoPE pipe flow facility are described in section 5, whereas section 6 raises some questions and comments on feasible measurements and related techniques for such a facility. The paper ends by giving our conclusions that can be summarized as: 'We believe that it is time to establish an international cooperation around a large-scale facility for turbulence research'.

2. What is a 'good' high Reynolds number experiment?

In the present context, we are interested in wall-bounded turbulence at high Reynolds numbers. The first question is then: how large must the Reynolds number be in order to be considered high? The second question is: which velocity and length scales are appropriate to define the Reynolds number?

In wall-bounded turbulence, the usual assumption is that the flow is governed by viscosity-influenced scales at the vicinity of the wall (for a smooth surface) that are usually called inner scales, whereas far from the wall the so-called outer scales are dominant. A high Reynolds number experiment should give a large enough separation between these two scales. In the following, we will look at length scales starting with the inner scale, which is usually taken as the viscous length scale

$$\ell_* = \nu/u_\tau$$

On the other hand, the outer scale may be taken as the boundary layer thickness (δ), the channel half-width (h), or the pipe radius (R). The ratio between the scales then becomes

$$\delta^+ = \delta/\ell_*, \quad h^+ = h/\ell_* \quad \text{and} \quad R^+ = R/\ell_*,$$

which may also be interpreted as the Reynolds number based on the friction velocity (u_τ) and the length δ, h or R, respectively.

Hence, the answer to the above second question is that δ^+, h^+ or R^+ should be a good definition of the Reynolds number. The answer to the first question cannot be given rigorously, but at least two possible viewpoints can be considered. One is to ensure a sufficiently large overlap region, where it is known that the mean velocity profile is logarithmic. The other viewpoint is that the Reynolds number should be high enough, so that a well-developed $k^{-5/3}$ region (k is the wave number) should be developed in the wave number spectrum. We will discuss these two viewpoints next.

2.1. Well-developed overlap region

In wall-bounded flows, it is well known that there is an overlap region of the mean velocity profile, where both the inner and the outer scales can be used. This region is well described by a logarithmic relationship

$$\frac{U}{u_\tau} = \frac{1}{\kappa} \ln y^+ + B,$$

between the mean streamwise velocity (U) and the distance from the wall (y). The two constants in the logarithmic relationship are the von Kármán constant (κ) and the so-called logarithmic intercept (B). There is strong evidence that in boundary layers, this region starts around $y^+ = 200$ and stretches out to approximately $0.15\delta^+$ (see Österlund *et al* 2000). In a pipe flow, we would expect the logarithmic region to stretch even further out since the wake component is known to be weaker in confined flows. If we accept that it starts at $y^+ = 200$ and want it to stretch over at least one decade of y^+ in order to have sufficient scale separation, we would like it to reach at least to $y^+ = 2000$. This would then directly lead to the conclusion that δ^+, h^+ or R^+ should each be at least 13 300 ($= 2000/0.15$)[8].

In order to have a sufficient range of the Reynolds numbers to be able to study scaling behavior, one needs to have a range over at least a factor of three; i.e. a Reynolds number ranges from 13 300 to 40 000. Therefore, we may assume that for pipes $R^+ = 40\,000$ is sufficient to provide a range of operations with adequate extent in the logarithmic overlap region.

For a pipe flow, we can easily calculate the Reynolds number based on the diameter and bulk velocity as $Re_\mathrm{b} = U_\mathrm{b}D/\nu = 2R^+U_\mathrm{b}/u_\tau$. A value of $R^+ = 40\,000$ corresponds to a bulk Reynolds number of more than 2×10^6. The corresponding Reynolds number based on the free stream velocity and momentum thickness (θ) for a zero pressure gradient (ZPG) turbulent boundary layer is around $Re_\theta = 1.2 \times 10^5$; i.e. nearly twice the highest values achieved in the experiments of Nagib *et al* (2007) and even larger than the highest Re_θ reached in the laboratory experiment by Knobloch and Fernholz (2002).

2.2. Well-developed $k^{-5/3}$ region

The Kolmogorov length scale is defined as

$$\eta = (\nu^3/\varepsilon)^{1/4}, \tag{2}$$

where ε is the local dissipation rate. According to the Kolmogorov theory, and based on local isotropy, there should exist a wave number region in the energy spectrum where the energy decays as $k^{-5/3}$. Near the wall, DNS data from turbulent channel flow (see the data base at http://www.murasun.me.noda.tus.ac.jp/turbulence/index.htm) show that there is only small variation in $\varepsilon\nu/u_\tau^4$ with the Reynolds number, whereas on the centerline, the normalized dissipation varies by

$$\varepsilon\frac{\nu}{u_\tau^4} \sim Re_\tau^{-1}. \tag{3}$$

Combining equations (2) and (3), we find that the ratio between the outer length scale h and the Kolmogorov scale η varies by

$$\frac{h}{\eta} \sim Re_\tau^{3/4},$$

whereas the ratio between the Kolmogorov scale and the viscous length scale becomes

$$\frac{\eta}{\ell_*} \sim Re_\tau^{1/4}. \tag{4}$$

[8] On the other hand, McKeon *et al* (2004) claim that mean velocity data from the so-called 'superpipe' indicate that a logarithmic region is only found for $y^+ > 600$ and $y/R < 0.12$. This would, with the same reasoning as above, give a minimum R^+ of 50 000 in order to have a logarithmic extent that would span a decade in +-units. At present, we have confidence in Österlund *et al*'s data, mainly because of the better spatial resolution of probes, however, this is an interesting discrepancy between the pipe and boundary layer observations that requires further investigation.

In order to have a fully developed $k^{-5/3}$ region, we would expect it to end around one-tenth of the wave number corresponding to the Kolmogorov length, to stretch at least over one order of magnitude in wave number space, and to extend down to scales an order of magnitude smaller than those for the energy containing eddies ($\sim h$). If by using the symbol $\ll$ we mean at least an order of magnitude smaller, then we could write this as

$$h^{-1} \ll \text{start of } k^{-5/3} \text{ region} \ll \text{end of } k^{-5/3} \text{ region} \ll \eta^{-1}.$$

From the numerical data base (which include the dissipation rate) it is possible to estimate η on the centerline and for $Re_\tau = 1020$, we find that $\eta_{\mathrm{CL}} = 5.5\ell_*$. By increasing the Reynolds number to 40 000 we would arrive at a value around $\eta_{\mathrm{CL}} = 13.7\ell_*$ using equation (4). Hence, in order to have a fully developed $k^{-5/3}$ region, it should end at 0.1 times the Kolmogorov scale, i.e. at around $(140\ell_*)^{-1}$, and stretch at least over one decade in wave number space down to $(1400\ell_*)^{-1}$. We would also expect the low wave number end of the $k^{-5/3}$ region to be an order of magnitude larger than the wave number corresponding to the (half-)height of the channel, which in this case is $40\,000\ell_*$. Hence the scale separation is fulfilled for this case.

In the case of a Reynolds number of $Re_\tau = 14\,000$, $\eta = 10.6\ell_*$ and again the criteria are fulfilled, although for $Re_\tau = 1020$ they are not. Actually, we can estimate that a minimum Re_τ of 10 000 is needed for these criteria to be met. Closer to the wall the dissipation increases, and hence, the Kolmogorov scale becomes smaller. Numerical simulations show that the energy containing scales also become smaller, and this may reduce the scale separation in this region. However, close to the wall the flow is far from isotropic so it may not be as important to satisfy the same criterion for the scale separation there.

In discussions related to CICLoPE, arguments similar to those presented above have been discussed based on the k^{-1} region of the spectra outlined in the work of Nickels *et al* (2005). The conclusions of these discussions are consistent with our estimates here that for a pipe flow reaching R^+ near 40 000, we have an adequate range of high Reynolds number turbulence.

Both the criteria discussed above, i.e. a well-developed overlap region or a well-developed $k^{-5/3}$-region lead to the conclusion that for pipe flow an R^+ of at least 40 000 is needed. If air is used as the flow medium, the Reynolds number can be increased by raising the density through pressurizing the gas, or by cooling the flow to very low temperatures as in cryogenic facilities; or alternatively by increasing the velocity or the size of the experiment. Another approach is to use a fluid with lower viscosity, such as water. However, one crucial point is that in order to accurately measure the turbulence fluctuations, with sufficient spatial resolution, the viscous scale has to be large enough compared to the sensing element size. Standard single hot-wire probes can be manufactured with a sensing length as small as 120 μm (with a wire diameter of 0.6 μm that ensures a length-to-diameter ratio of the sensing element of 200). It is also recognized that probe lengths larger than $10\ell_*$, may lead to spatial averaging, which then sets a lower limit for the viscous length of about 12 μm. To reach a Reynolds number of 40 000 we arrive at the required radius of the pipe from equation (1), which yields a radius of 0.48 m, or a diameter of 0.96 m. According to Zagarola and Smits (1998), a length of the pipe of at least $100D$, or nearly 100 m, would be necessary to achieve a fully developed pipe flow for these Reynolds numbers.

3. Recent high Reynolds number experiments

Here, we discuss and briefly describe facilities used for some recent high Reynolds number experiments in wall-bounded flows that may be considered classical or canonical; i.e. circular pipe flow, two-dimensional (2D) channel flow and flat-plate boundary layer flows. To these

we also add atmospheric boundary layer flows from which recently new results have been reported. We exclude the plane Couette flow, although clearly it is one of the canonical flows, since no high Reynolds number experimental data exist for that case.

3.1. Pipe-flow experiments

A unique advantage of the pipe flow compared with all the other canonical cases mentioned above is that the wall shear stress can be determined directly from the pressure drop along the pipe, which usually can be measured quite accurately. One of the crucial design features of a pipe-flow experiment is the length-to-diameter ratio (L/D) of the pipe itself. This issue was discussed by Zagarola and Smits (1998) who argue that there are two different processes that have to take place: firstly, the length required for the boundary layer growth such that the boundary layers reach the center of the pipe; secondly, the length required for the turbulence to become fully developed. Both lengths increase with the Reynolds number; i.e. the higher the Re, the larger the pipe L/D has to be.

Over the years, there have been a number of pipe-flow experiments reported in the literature, but they are mainly at low Reynolds numbers and do not fulfill the criteria discussed in section 2. A well-recognized high Reynolds number pipe-flow experimental facility has become known as the Princeton superpipe (see Zagarola and Smits 1998). The pipe has a diameter of 129 mm and a length of 26 m. The corresponding L/D is hence more than 200 and the flow is expected to be fully developed even at the highest Reynolds numbers of the facility ($Re_D = 35 \times 10^6$). The high Reynolds number is obtained through pressurizing the air up to pressures of 187 bar. In this way Reynolds numbers (R^+) of up to 500 000 have been achieved. Although the Reynolds numbers that are achieved in the superpipe are extremely high for a laboratory experiment, it is on the expense of a very small viscous length scale, i.e. for $R^+ = 500\,000$ the viscous length ℓ_* is only slightly above 0.1 μm. The scientific results from the superpipe have been presented in a number of papers since 1998 and include measurements of the mean velocity distribution and new information on the skin friction variation for both the smooth and rough surfaces. However, due to the spatial resolution limitations, few reliable turbulence data have been published.

In figure 1, the range of various pipe experiments in terms of the viscous length scale (ℓ_*) as a function of the Reynolds number (R^+) is plotted. The experiments include air, compressed air and water as flow medium, but their interrelated relation is a line with the slope -1, according to the relation $\ell_* = R/R^+$ and this is independent of the flow medium. As can be seen, most experiments are for low Reynolds numbers. The superpipe covers a wide range of Reynolds numbers but does not pass through the range of interest that was defined in section 2.1; i.e. $R^+ > 13\,300$ and $\ell_* > 10$ simultaneously. In the figure, we also plot the range for the planned CICLoPE pipe. Although this experiment will have a much smaller Reynolds number range than the superpipe it is designed such that the scales within that range will be large enough to be reasonably well resolved by present measurement techniques.

3.2. Channel flow experiments

There are two channel flow experiments, at low-to-moderate Reynolds numbers, from which turbulence data have been reported recently. One is located at the Institute of Fluid Mechanics, Friedrich-Alexander-Universität Erlangen-Nürnberg and detailed specifications can be found in Zanoun *et al* (2003). The channel height is 50 mm, its width 600 mm and its length 6500 mm. The flow medium is air. Measurements have been reported for Reynolds numbers Re_τ up to 4783. The results from this facility have relied primarily on hot-wire and pitot probe measurements, and oil-film interferometry data.

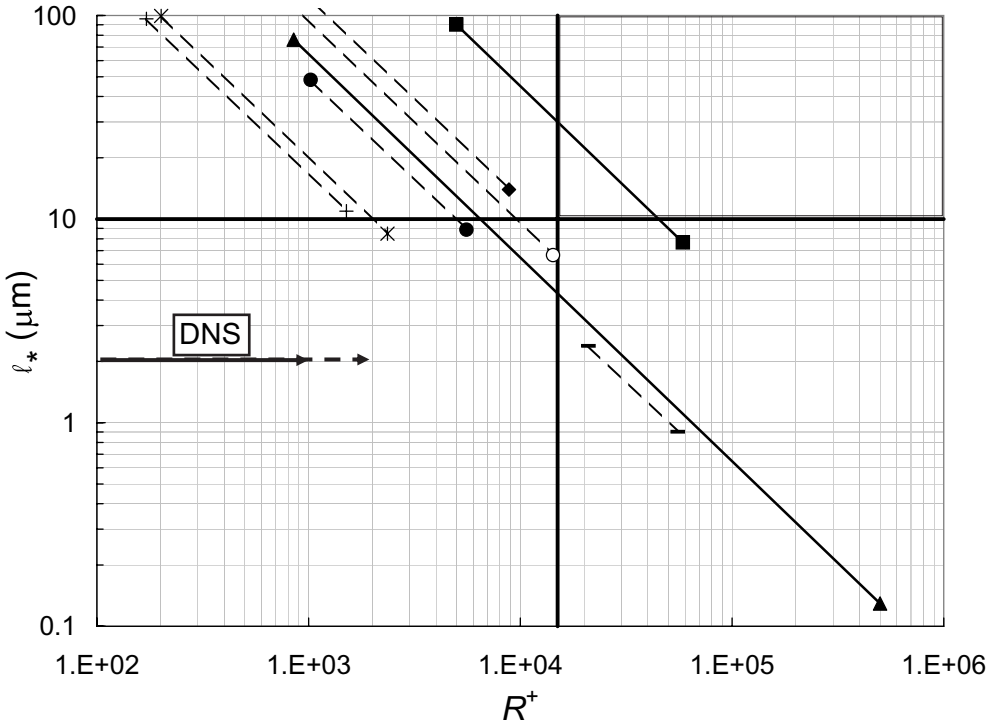

Figure 1. Range of Reynolds number and viscous length scale of various pipe-flow experiments. □: Wygnanski and Champagne (1973), air, $D = 0.033$ m; △: van Doorne and Westerweel (2007), water, $D = 0.040$ m; •: Monty (2005), air, $D = 0.0988$ m; ▲: Zagarola and Smits (1998), compressed air, $D = 0.129$ m; ×: Nikuradse (1932), water, $D = 0.10$ m; ○: University of Cottbus (under construction), air, $D = 0.19$ m; +: Laufer (1954), air, $D = 0.123$ m; ■: CICLoPE experiment, air, $D = 0.90$ m. The highest Reynolds number for a DNS reported so far for turbulent pipe flow is the one by Satake *et al* (2000) at R^+=1050. For turbulent channel flow, Hoyas and Jiménez (2006) have reported a DNS at $h^+ = 2003$. The solid vertical line refers to the criterion of a well-developed overlap region ($R^+ > 13\,300$, see section 2). Horizontal line gives the limit for $\ell_* > 10\,\mu$m that is the minimum for sufficient spatial resolution. Hatched region of the upper right corner shows where the criteria for both spatial resolution and high enough Reynolds number are met. As seen the CICLoPE experiment is designed to work in this region.

A second channel flow facility located in the USA has been described by Christensen and Adrian (2001). Dimensionwise it is similar to the one in Erlangen; it has a height of 50.8 mm, a width of 514 mm and a development length of 5500 mm. It also has air as a flow medium and has been primarily used for PIV measurements. The highest Reynolds number reported was 1734. A third channel (100 mm high, 1170 mm wide and 20 500 mm long) is located at the University of Melbourne. Although it is capable of nearly doubling the highest Reynolds number achieved with the other two channels, no published data are readily available. Q3

We should also point out that the Reynolds numbers achieved through DNS of channel flow, although still below that obtained in experiments, are steadily increasing. For instance, the one reported by Abe *et al* (2004) had a Reynolds number of 1020 and the one by Hoyas and Jiménez (2006) was as high as 2003. The results from the DNS have compared favorably with measurements from the two channel experiments described above, and confirm the need for higher Reynolds number experiments with improved spatial resolution.

3.3. Wind tunnel boundary layer experiments

Two closed-return wind tunnels, in which high quality, high Reynolds number boundary layer experiments have been carried out during the last decade, are the MTL wind tunnel at KTH, Stockholm and the National Diagnostic Facility (NDF) wind tunnel at the Illinois Institute of Technology, Chicago. It is interesting to note that the principal investigators of the turbulent boundary layer studies in these two tunnels (Johansson and Nagib, respectively) have been cooperating, and in some of the resulting publications also used data from both tunnels to strengthen the line of arguments (see, for instance, Nagib *et al* 2007, Österlund *et al* 2000).

Q4

The MTL wind tunnel has an overall length of 25 m and test section dimensions of $1.2 \times 0.8 \times 7.0\,\mathrm{m}^3$ (width × height × length). The contraction ratio is 9 : 1, a heat exchanger controls the temperature, and the maximum speed (with empty test section) is $69\,\mathrm{m\,s}^{-1}$. For turbulent boundary layer experiments, a flat plate is mounted 20 cm above the tunnel floor, and measurements can be carried out along the full-length of the plate. The leading edge is elliptical and the boundary layer is tripped about 20 cm downstream the leading edge. For high Reynolds numbers, the most useful measurement position is at a station 5.5 m downstream the leading edge with free stream velocities up to $50\,\mathrm{m\,s}^{-1}$. Under these conditions, Re_θ is approximately 27 000 and the corresponding δ^+ is around 6000.

The NDF at the Illinois Institute of Technology has a $1.52 \times 1.22 \times 10.3\,\mathrm{m}^3$ test section, and is capable of reaching a maximum free-stream velocity of $110\,\mathrm{m\,s}^{-1}$ (see also http://fdrc.iit.edu/facilities/ndf.php). The flow quality is controlled by a honeycomb, six screens and a 6 : 1 contraction upstream of the test section. The resulting free-stream turbulence intensity is $<0.05\%$ at all velocities. Turning vanes in two turns of the tunnel are used as heat exchangers for regulating the free-stream temperature, and the turning vanes in one turn are lined with acoustically absorbent material to dampen acoustic disturbances. The test section itself is a modular design and its design and long length allow it to be modified to establish various pressure gradients (both adverse and favorable) by adjusting the height of 17 ceiling panels over the length of the boundary layer plate. The flat plate, which spans the width of the test section, measures approximately 10.8 m from the leading edge to the end of a flap. The plate is suspended 0.52 m above the tunnel floor. Transition triggers in the form of 'V'-notched strips are located between 8 and 25 cm from the leading edge.

Turbulent boundary layer experiments in the NDF have been performed for five different pressure gradient cases over a flat plate, including the ZPG case (see Nagib *et al* 2006, 2007). The measurements for all pressure gradient cases were acquired at six streamwise locations; i.e. $x = 3.8$, 4.6, 5.5, 6.4, 7.3 and 9 m. For the ZPG measurements, the free-stream velocity at the leading edge was kept at $U_0 = 30$, 40, 50, 60, 70 and $85\,\mathrm{m\,s}^{-1}$, whereas for the pressure gradient cases upstream free-stream velocities of $U_0 = 40$, 50 and $60\,\mathrm{m\,s}^{-1}$ were utilized. The highest achievable values for ZPG boundary layers in the NDF are Re_θ of approximately 70 000 and the corresponding δ^+ of about 15 000.

In both MTL and NDF tunnels the oil-film interferometry method has been used to obtain an independent measurement of the wall shear stress, whereas various hot-wire and pressure probe measurements have been used for determining the mean and fluctuating velocity components.

3.4. Atmospheric boundary layer experiments

The use of the atmospheric boundary layer as a test facility is, of course, an interesting possibility in order to reach high Reynolds numbers and still have good spatial resolution. Only a few types of terrain are useful if one wants to have a boundary layer over smooth-wall conditions. Measurements from two different types of sites have recently been used for

boundary layer studies: one site is located in the Utah Great Salt Lake Desert (Kunkel and Marusic 2006), the other measurements are from observations over sea ice in the Antarctic and Arctic regions (Andreas *et al* 2006). There are many difficulties associated with these types of measurements, however, they give access to boundary layers of unprecedented high Reynolds numbers. The boundary layer thickness is typically larger than 100 m, whereas free-stream velocities are of the order of 10–20 m s^{-1}. Hence, the Reynolds number based on boundary layer thickness is of the order of 10^8 or larger.

In the experiments of Andreas *et al* (2006), the idea was to determine the Kármán constant from measurements in the logarithmic layer. The velocity measurements were made with propeller and sonic anemometers. In contrast to laboratory experiments, a large number of profiles were measured under various conditions (wind speed, wind direction, thermal stability, etc) and velocity data from approximately 10^3 h of measurement time were available. The results show that individual profiles have a large scatter in the values of the Kármán constant. However, the individual values of the Kármán constant can be averaged and a mean value has been reported by the authors. The variation among individual profiles may depend on various reasons; one is probably that the averaging times at each measuring location need to be large in order to achieve good statistical accuracy of the individual mean (see section 6 for further discussion about this issue).

On the other hand, Kunkel and Marusic (2006) used hot wires for their measurements and these experiments have a scope similar to what would be carried out in a wind-tunnel investigation. In the Utah desert site it seems harder to get a boundary layer under neutral conditions, and hence, the available measurement time is limited. They present turbulence data of the streamwise and normal velocity components in the logarithmic layer, as well as spectra that show the $-5/3$ region over at least two decades in wave number.

4. Research issues for a high Reynolds number flow facility

In the following sections, we will outline a preliminary set of potential scientific objectives to be investigated at the CICLoPE. The following sample objectives are based on the outcome from a workshop held in Bertinoro, Italy, during September 2005. The full text for the objectives can be found at the homepage of the CICLoPE project (http:// www.ciclope.unibo.it), and the names of some of the key individuals who contributed ideas to the objectives are mentioned in the acknowledgment section of this paper.

4.1. Large-scale structures and energy transfer in wall-bounded shear flows

Wall-bounded flows are characterized by a hierarchy of organized eddying motions occurring on different spatial and temporal scales. The near-wall region contains a multitude of quasi-streamwise vortices, which induce organized structures of slow and fast moving fluid. The kind of structures that populate the outer region is less established. Basically, they are described as packets of hairpin-like vortices, or alternatively as large-scale low-momentum regions, which manifest coherence on scales comparable with the external dimension of the flow. For a long time, there have been suggestions of a coupling between near-wall dynamics and large structures, and recent numerical simulations seem to confirm this. In this case, near-wall regeneration events would be locked to the specific sites determined by the large-scale structures and by their slow dynamics.

From a statistical point of view, it is not clear that which kind of mechanism may induce such inner–outer scale coupling, leaving open the issue of the origin of the large-scale features. A tool able to deal with this question is provided by the scale-by-scale balance of kinetic

energy (see e.g. Marati *et al* 2004). It would discern between the different mechanisms which may participate in feeding a given scale of flow motion; namely, local production by coupling with the mean shear, spatial fluxes and direct/inverse energy cascade across scales.

To further investigate this issue an experiment that guarantees access to widely separated scales of motion is needed. Various measurement techniques should be used, both standard methods, such as multipoint hot-wire anemometry but also highly sophisticated measurement techniques, as for example dual-plane stereo image velocimetry will be useful in this context.

Also the novel technique utilized by Tsuji *et al* (2007), where fluctuating pressure can be measured inside the wall-bounded flow, may prove to be very effective here. This technique, which currently is being further developed to increase spatial resolution, gives new possibilities to study key elements of inner–outer scale interactions through pressure root mean square (rms)-distributions and their scaling behavior. In addition, but perhaps not as important, this technique can be used to examine the scaling behavior of two-point pressure–velocity correlations.

4.2. Anisotropy and SO(3) decomposition

One of the basic aspects of turbulence theory concerns the recovery of isotropy in the small-scale range, which is a real challenge to theoreticians, especially for turbulent wall-bounded flows. Actually, boundary layers display a variety of different behaviors, ranging from the outer part of the logarithmic region, where a classical inertial range is well established, down to the inner part of the log-layer/outer part of the buffer region, where anisotropy may penetrate within the dissipation scales. This issue has a large impact in all the applications that require simulations of wall-bounded turbulent flows.

In this context, there are still several open questions:

- How is isotropy recovered as a classical inertial range is approached?
- Are scaling laws preserved in some generalized sense even in conditions which are relatively far from purely isotropic conditions?
- What are the detailed mechanisms driving the isotropization of the small scales?
- Are there aspects of the behavior of the anisotropic scales in the production range which manifest universality?
- Can we develop a theoretical framework to describe the statistics of fluctuations at production scales?

Recently, the so-called SO(3) decomposition has been applied to gain some understanding of part of the issues raised above (see e.g. Jacob *et al* 2004 and references therein). It makes it possible to express structure functions as a sum of components arranged into a hierarchy of increasingly anisotropic contributions with the aim of understanding how turbulence changes from anisotropy-dominated fields on the large scales to the isotropy at small separations. Most available results deal with mild perturbations of isotropic statistics, but the same theoretical tools can be used to address strongly anisotropic flows as well. In this respect, the preliminary evidence from numerical simulations and experiments is strongly encouraging, though suffering from the shortcoming of facilities unable to explore the fine structure of turbulence at high Reynolds numbers.

4.3. Inner/outer scaling of spectra, correlations and other high-order statistics in various regions

The spectra of turbulent flows and the correlation functions are very important since they can be used to separate the effect of different scales, or sizes, of motions that contribute to the

dispersion of contaminants, the surface friction and the heat transfer from the surface. Such information is essential in developing a better understanding of the underlying physics of the flows and developing accurate predictive models, applicable to the high Reynolds number flows typical of engineering applications and natural processes.

Measurements have been made of the spectra in a variety of laboratory experiments and also in the atmospheric boundary layer. Unfortunately, although useful, measurements from these two flows are limited for different reasons. The vast majority of laboratory measurements have been limited to moderate Reynolds numbers due to the limited size of typical facilities. The spatial resolution of measurements at higher Reynolds numbers in the laboratory is also limited, again due to the limited size of the facilities. One such scaling experiment at moderately high Reynolds numbers was reported by Österlund *et al* (2003); however, for the scaling results to be conclusive a larger range of Reynolds numbers would be desirable.

Measurements in the atmospheric boundary layer do not suffer from these limitations and it is possible to attain excellent spatial resolution at very high Reynolds numbers. However, atmospheric measurements are problematic as the experimentalist has no control over the flow conditions, and varying conditions make it difficult to obtain converged statistics.

Accurate scaling experiments hence need a controlled high Reynolds number laboratory experiment to eliminate several controversies presently related to the correct scaling of spectra and correlations. Also the scaling of other statistical features of wall-bounded turbulence may be studied in such a facility, such as the scaling of the turbulence intensity in the buffer region with Reynolds number (see e.g. Metzger and Klewicki 2001). A high Reynolds number facility would also be able to further verify the k^{-1} spectral law discussed by Davidson *et al* (2006).

4.4. Evidence on non-universality of the Kármán constant, and other scaling anomalies

The separation in scale size between the inner, or wall scales, and the outer scales determined by geometrical constraints increases with the increasing Reynolds number. This separation is what gives the characteristic two-layer feature of wall bounded flows, therefore, in order to increase our understanding of turbulent flow physics it is essential to obtain accurate data from several well-established and documented high-Reynolds number flows. The asymptotic shape of the mean velocity distribution in the overlap region, that connects the inner and outer regions, is a key element in our understanding of wall-bounded turbulence.

Recently completed flat-plate boundary layer experiments at the high Reynolds numbers, $Re_\theta > 10\,000$, in presence of adverse and favorable pressure gradients, have been used to evaluate the mean velocity profiles in the overlap region (Nagib *et al* 2006). The profiles exhibit the logarithmic behavior of the mean velocity in the overlap region in a similar way to the well-documented case of ZPG. In contrast to the ZPG case, the pressure gradient cases exhibit systematic variations in the parameters describing the overlap region, namely, the Kármán coefficient κ and the additive term B, which are believed to be *constant* based on classical arguments.

The variations in κ and B are not only exhibited for the clearly non-equilibrium cases of strong favorable pressure gradient (SFPG; $\beta \approx -0.15$) and complex pressure gradient (CPG), but also for the mild adverse and favorable pressure gradient cases, APG ($\beta \approx 0.1$–0.3) and FPG ($\beta \approx -0.09$––0.15), respectively. The variations for APG and FPG are opposite in nature when referred to the equilibrium state of a ZPG turbulent boundary layer. The results are also self consistent and in agreement with fully developed pipe and channel flows where κ values higher than we find for ZPG are measured; $\kappa \approx 0.41$ compared with 0.384.

The non-universality of Kármán coefficient κ is not only of scientific importance but also has a major impact on the prediction of turbulence using various closure models. All of the currently used models rely on the hypothesis that κ is a constant; often taken to be equal to its most popular value of 0.41. The use of a circular diverging test sections in a pipe-flow experiment, to include ZPG, or converging segments of a 'pipe' can be used for further confirmation of these trends.

In addition, the recent high Reynolds number data revealed another limitation of the classical theory at all finite Re_θ values. Nagib *et al* (2007) suggested after careful assessment of data over a very wide range of Reynolds numbers, that (at least) two outer length scales are required to fully describe the mean velocity profile in a ZPG TBL. One can think of these two outer scales as being associated with the boundary layer thickness and the streamwise growth of the boundary layer thickness. They suggest that it is only at infinite Reynolds numbers that the ZPG TBL reduces to a two-scale problem with one inner scale and one outer scale as in the classical theory. In contrast, a fully developed pipe flow is homogeneous in the streamwise direction, and should therefore, insure a single outer scale and the unique opportunity to examine other asymptotic trends of the mean flow at finite but high Reynolds numbers.

4.5. Small deviation of canonical scaling laws using approximate symmetries/Lie groups

In recent years, it became clear that at least for 'clean' canonical turbulent flows, such as pipe, channel or boundary layers, the group theory provides the axiomatic building block for deriving turbulent scaling laws. The basis of the analysis is the infinite set of multipoint correlation equations that solely originate from the Navier–Stokes equations. Applying group theory invariant solutions (scaling laws in turbulence) for wall-bounded shear flows have been obtained without any closure assumption. In fact, it turned out that the von Kármán logarithmic law of the wall is by no means the only nontrivial self-similar mean velocity profile which may be given explicitly. The set of mean velocity profiles obtained includes an algebraic law in the center of a channel flow, the linear mean velocity in the center of a Couette flow, the linear mean velocity in the center of a rotating channel flow and an exponential mean velocity profile. The exponential law in particular has not been previously reported in the literature. Besides the original work of Oberlack (2001) it is shown by Lindgren *et al* (2004), using the high Reynolds number KTH data base as well as DNS data in Khujadze and Oberlack (2004), that such a law describes the outer part of a boundary layer flow over a flat plate and is, in fact, an explicit form of the velocity defect law.

All the latter classical and new scaling laws were, however, derived under idealized and rather 'clean' conditions. In particular, infinite Reynolds number and the absence of a pressure gradient was presumed. Further, a fully parallel flow in the mean sense was conjectured which is not true for boundary layer flows.

For almost two decades Reynolds number dependence of turbulent scaling laws has been under intense debate and, in fact, recently also pressure-gradient dependence and non-parallel effects have been observed (see Nagib *et al* 2006). Though these effects appear to be of higher order, i.e. they may not change the global functional behavior of the scaling laws they still significantly influence the scaling parameter such as the von Kármán constant κ in the logarithmic law of the wall.

A new development is to introduce approximate group theory to derive the turbulent scaling laws which may depend on a small parameter such as those mentioned above. Approximate groups provide a new mathematical methodology which unifies group theory with regular asymptotics. Hence, it gives the ideal framework to tackle tasks, e.g. to derive the

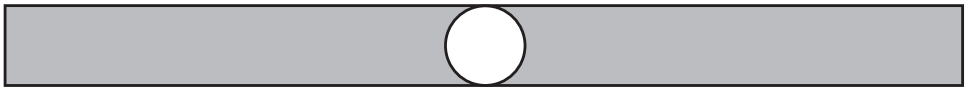

Figure 2. Comparison between cross-section area of pipe and channel flow. A channel with an aspect ratio of 12 has a cross section which is 15 times larger than a corresponding pipe flow.

pressure-gradient dependence of the von Kármán constant κ. The key advantage of the new method is that certain physical parameters such as the pressure gradient, which are under idealized conditions are symmetry breaking, i.e. no exact scaling law exists, can now be mathematically handled at least in an asymptotic sense.

In order to thoroughly validate these types of scaling laws for both the effect of pressure gradient and Reynolds number dependence, high Reynolds number experimental data are needed.

5. Design features of pipe-flow facility at CICLoPE

The idea of a collaboration between several researchers from different universities on a high Reynolds number flow facility located in Predappio was conceived during a visit by Hassan Nagib and Alessandro Talamelli to KTH in 2004. As seen in section 3, many attempts have been made to create large-scale experiments but so far they have been limited in one way or the other. The use of a pipe as compared with, for instance, a parallel-walls channel is advantageous in two ways, both with respect to the cost of construction and the flow rate needed. Recent channel flow experiments have used aspect ratios around 1:12 in order to ensure a sufficiently wide central region without the influence from the side walls. Such a channel has a cross-stream area about 15 times larger than a pipe with a diameter of the same dimension as the channel height. Hence, to obtain the same Reynolds number based on diameter or height the flow rate would have to be some 15 times larger in the case of the channel (see figure 2). Also, the construction costs and space requirements would increase nearly proportionally in case of the channel.

5.1. Special requirements for a long-pipe-flow experiment

The design of a long-pipe-flow facility is non-standard and a large number of requirements has to be met. In the following, we describe various criteria and discuss the design features of the facility as they are known today (May 2007). In principle, a long pipe flow facility can be designed in a similar way as a wind tunnel. However, there are two main differences: the pressure drop is much larger in the test section and the pipe is in itself the test section. These characteristics put extra demands both on the fan, which has to provide the desired flow rate against a higher pressure drop, and on the pipe itself which must satisfy some strict requirements, e.g. geometric tolerances, surface finish and alignment.

5.2. The laboratory

The laboratory for CICLoPE is located in Predappio, Italy, besides the old factory of the *Caproni Industry*, which was one of the major sites of aircraft production during the period 1930–1945. The site in Predappio was built after the First World War to improve the airplane production in Italy, and it became operative in 1935. After 1940, it was successively improved in order to boost its productivity and fulfill the needs during the Second World

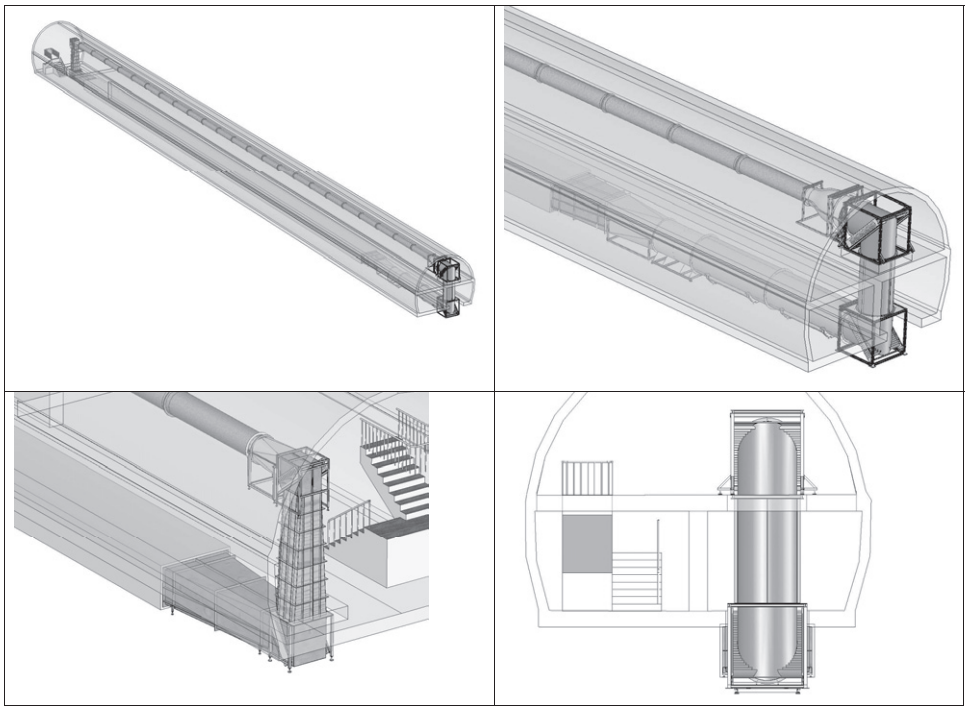

Figure 3. Outline of the long-pipe facility. Figures clockwise from upper left. a) Full-length of the pipe located in the tunnel, (b) close-up of the third and fourth corners and the contraction before the start of the pipe, (c) cross section of the pipe facility and the tunnel showing the third and fouth corners and (d) the end of the pipe with the diffuser and test section.

War. It was during this period that a tunnel complex was excavated, in order to provide both shelter for civilians, and make the plant operative even under bombing activities. After 1944, the Predappio site was gradually vacated and all the equipments moved to sites located farther north. The tunnels were subsequently occupied by Allied forces until 1946 and then finally transferred to the Italian *Aeronautica Militare*. In 2006, the tunnels were given to the *University of Bologna* specifically for the CICLoPE laboratory.

The complex comprises two 130 m long tunnels with a diameter of about 9 m each. The two tunnels are linked together and to the exterior by two perpendicular galleries of a smaller size. The space available in these tunnels is not restricted to the long-pipe experiment, but allows enough room for future developments and for other experiments. The section of the first tunnel is separated in two floors. The long-pipe facility will be set on the upper floor and the return circuit will be located under the ground floor of the tunnel as shown in figure 3. This layout has been chosen as the best compromise in terms of cost, accessibility, security and space for future developments.

5.3. The facility

The present configuration of the experimental set-up is the result of a preliminary design phase. Hence, some elements could still change in terms of dimensions and material until the end of the final construction. The facility is basically a closed-loop wind tunnel operating with air at atmospheric pressure. A closed loop has been chosen since it will allow the

flow characteristics to be accurately controlled. The layout resembles an ordinary wind tunnel where the main difference is the long test section which gives most of the friction losses. However, many of the various aerodynamic components are the same as those for an ordinary wind tunnel (corners, diffusers, screens, contraction, etc), and for several of these components we relied on the recent experience gained when constructing the MTL and BL-wind tunnels at KTH Mechanics, Stockholm. In the following, we describe the facility starting downstream of the test section and following the flow loop around the circuit (again see figure 3).

The expansion part linking the test section to the return flow section will have two expanding corners of rectangular cross section with an expansion ratio of 1.3 based on the design of Lindgren *et al* (1998). This will achieve a substantial part of the required total expansion of the flow already by the beginning of the lower return duct. After the second corner, a two-dimensional diffuser expands the flow laterally to the full width along a return section. At the end of this return section, a two-dimensional contraction followed by a square to circular converter brings the air into the fan.

A heat exchanger located at the end of the return flow section just upstream of the contraction, where the mean air velocity is the lowest, will accurately control the air temperature in the pipe. The mixing produced by the fan will ensure a thermal homogeneity of the flow after the heat exchanger. The aim is to keep the flow temperature variation in the test section less than 0.1 °C.

The fan is of the single-stage type, with a diameter of 1.8 m, and has 12 blades specifically designed for this experiment. The fan is designed to produce 3.5 kPa of pressure difference with a volume flow rate of 38 $m^3 s^{-1}$. It will be powered by a 250 kW ac-motor controlled by a frequency converter for accurate velocity control. The section between the fan and the settling chamber will have a circular cross section of constant area. A 11 m long straight pipe downstream of the fan will be coated with noise absorbing material to reduce the noise produced by the fan and to allow the wake of the fan to decay before the corner.

The two last corners are non-expanding with circular cross sections, and are separated by a straight fiberglass tube. Finally, the settling chamber and contraction will be made of fiberglass, and will incorporate a honeycomb and three screens to homogenize the flow before the settling chamber, and to reduce the turbulence intensity. The shape of the contraction will be similar to the one used in the MTL wind tunnel, which was designed using inviscid/boundary layer calculations to optimize the pressure gradient along the contraction walls. The contraction will have a length of 2.6 m and a contraction ratio of four with diameters of 1.8 and 0.9 m for the inlet and outlet, respectively.

The main part of the set up is the long pipe. It consists of a 115 m long tube with an inner diameter of 0.9 m. The pipe will be made of 5 m long modules held on concrete blocks by precision positioning elements. The pipe modules are made of carbon fiber with flanges at both ends for precise junction of the elements. The main test section, at the end of the pipe, will have optical access for PIV and local density approximation (LDA) as well as various traversing systems for different sensor types.

5.4. Pressure drop

The distribution of the pressure drop along the circuit is shown in table 1 and the corresponding power factor is shown in table 2. As it can be seen, 78% of the pressure drop is generated by the friction in the pipe, which also makes the power factor quite high as compared to the value for a typical wind tunnel. The total pressure drop in the circuit is about 3500 Pa at a mean velocity of 60 m s^{-1} in the pipe.

Table 1. Percentage of pressure losses at a 50 m s^{-1}.

Element	% losses
Main pipe	78.04
Section converter	1.19
Corner 1 (expanding)	2.25
Vertical diffuser	1.93
Corner 2 (expanding)	0.47
Two-dimensional diffuser	1.09
Return duct	1.62
Cooling system	0.16
Two-dimensional convergent	0.02
Section converter	0.08
Circular pipe	0.25
Corner 3	0.18
Vertical part	0.07
Corner 4	0.18
Honeycomb	0.25
Screens	11.64
Settling chamber	0.01
Contraction	0.54

Table 2. Power factor.

$\overline{U}$ (m s^{-1})	Power factor at various mean velocities
5	2.52
15	1.96
30	1.75
45	1.67
60	1.61

5.5. Critical requirements

5.5.1. Surface roughness. The mechanical requirements for the pipe are mainly fixed by the demand to have a hydrodynamically smooth surface. In order to achieve this, the sand equivalent surface roughness of the pipe k_s has to be lower than $3.5\ell_*$ according to recent results by Shockling *et al* (2006) for a honed finished surface. They also showed that for such a surface $k_s/k_{rms} \simeq 3$. As specified earlier the minimal scale for spatial resolution for the long pipe is $\ell_* = 10\,\mu$m, which translates into an rms surface roughness of maximum 12 μm. With the proposed carbon fiber pipe modules the surface roughness will be well below this value.

5.5.2. Diameter accuracy. The absolute accuracy of the pipe diameter is not very stringent as long as its variations are small along the pipe. High-flow-quality wind tunnels such as MTL at KTH in Stockholm or NDF at IIT Chicago have mean velocity variations $\Delta U/U_0$ of the order of 0.2%. For a pipe flow one can write

$$\frac{\Delta U}{U_0} = \frac{\Delta S}{S} = 2\,\frac{\Delta D}{D}, \tag{5}$$

where S is the cross-section area of the pipe and D its diameter. To get similar flow quality, the diameter variation for a diameter of 0.9 m is

$$\Delta D \leqslant \frac{\Delta U}{U_0}\,\frac{D}{2} = 0.9 \times 10^{-3}\ \text{m}. \tag{6}$$

Table 3. Flow quantities of interest in wall-bounded high Reynolds number experiments and possible measurement techniques/methods.

Flow quantity	Mean value	Fluctuations
Flow rate	Pressure drop across	–
	contraction or screens	–
Pressure		
Absolute pressure	Barometer	–
Pressure drop	Pressure taps	–
Wall pressure	Pressure tap	Microphone
		Pressure transducer
		Porous PSP
Static pressure in flow	Pressure probe	Tsuji probe
Dynamic pressure	Pitot tube	–
Wall shear stress		
	Preston tube	–
	Oil film interferometry	–
	Balance	micro balance (MEMS)
		Micro pillars
	Laser fan	Laser fan
	Velocity profile in viscous sublayer	Hot wire on the wall
Velocity		
	Hot wire	Hot wire
	LDV	LDV
	–	PIV
Temperature		
	Cold wire	Cold wire
	Pt100	

6. Critical and feasible measurements

A modern flow experiment employs a variety of measurement techniques that can be utilized and for each technique several different configurations may be required. A compilation of various flow variables of interest and measurement techniques available is given in table 3.

In order to conduct high-quality experiments, at least two requirements have to be fulfilled, viz a high-quality flow facility and suitable measurement resources. Therefore, it is important already at the planning stages of the project to get an idea of what accuracy is needed and to establish what quantities should be measured. In terms of accuracy there are a number of different aspects to be considered as listed below:

- drift
- noise (electrical, vibration and sound)
- AD converter (resolution, sample and hold)
- accurate positioning and traversing
- averaging time
- spatial resolution
- frequency resolution
- wall effects
- particle dynamics.

The first five listed are general problems for most measurement systems but are important to address for high- quality measurements. Spatial and frequency resolutions are probe and/or

instrument dependent, whereas wall effects are problems arising from interference between the wall and the probe. For intrusive methods (i.e. probe measurements), it is not only the probe interference that may constitute an error source but also the blockage of the traversing system may also result in disturbances. The question whether particles follow the flow accurately is, however, a question only for non-intrusive methods which use the particles to determine the flow speed.

Earlier turbulence research has mostly relied on point measurements, i.e. measurements at one point at a time, whereas for many situations two or multipoint measurements are needed. With PIV also field measurements in a plane are possible and with stereoscopic PIV all three velocity components can be measured simultaneously.

For measurements using indirect measurements, such as hot-wire anemometry, the accuracy of the measurements cannot be higher than the accuracy of the calibration which implies that the calibration set-up is as important as the measurements themselves and has to be designed accordingly.

The standard quantities that should be considered in a turbulence experiment should comprise the following quantities and distributions of all three velocity components:

- mean velocity distribution
- turbulence intensity (rms) distribution
- distribution of higher moments
- probability density distributions (pdf)
- spectra (wave number and frequency)
- correlations (spatial and time).

To ensure the desired accuracy in the results, it will be essential to have and perhaps to use at the same time complementary means for measuring mean and turbulence quantities.

6.1. Spatial resolution issues

The accuracy and representation of all measurement techniques are dependent on what may generally be referred to as the probe size or volume. Velocity measurements using hot wires, LDV, PIV and other methods are particularly affected by such spatial averaging or resolution.

For single hot wires, it is the length of the hot-wire sensor which is the critical dimension, and the smallest probes which are convenient to use have a wire length of the order of 250 μm with a sensor diameter of 1.2 μm. However, it is possible to use wires with a diameter of 0.6 μm, thereby allowing us to reduce the length to 120 μm. Various studies have shown that probes with a spanwise length larger than about $10\ell_*$ lead to spatial averaging effects, which indicates that the smallest viscous length should be larger than about 10 μm in order to be able to resolve the turbulence without significant effects of spatial averaging.

Another approach to accurately measure averaged quantities relies on repeated measurements with probes of different small sensing elements and extrapolation of the data down to much smaller scales. i.e. the desired quantity can be measured with several probes of different but not too large sensing lengths and then the results are extrapolated to a zero sensing element size. The extrapolation can become quite accurate if it is combined with theoretical knowledge about the effect of the spatial averaging. Even time-resolved measurements can be corrected if such measurements are carried out simultaneously (in virtually the same position) with two probes of different spatial extent. This may be hard to achieve but could be tried with for instance two parallel hot wires.

6.2. Time-averaging issues

When averaging a stationary turbulent signal the accuracy of the average depends on the averaging time (see, for instance, Sreenivasan *et al* 1978). It is possible to show that the relative error (ϵ) for the determination of the mean value becomes

$$\epsilon = \left(2\frac{\Lambda}{T}\right)^{1/2} \frac{u_{\rm rms}}{\overline{U}}, \tag{7}$$

where Λ is the integral timescale of the turbulence. This result gives a useful estimate of how long we need to sample in order to get a specified accuracy. For instance if we want an accuracy better than 1% we should sample for at least

$$T(\epsilon < 1\%) > 2\Lambda \left(\frac{u_{\rm rms}}{\overline{U}}\right)^2 \times 10^4.$$

As an example, consider measurements of the streamwise velocity at various radii in a turbulent pipe flow experiment with air as the flowing medium and with $U_{\rm CL} = 30\,{\rm m\,s^{-1}}$. The diameter ($D = 2R$) of the pipe is 0.9 m. The maximum local level of $u_{\rm rms}/U$ is 0.40, which occurs within the viscous sublayer close to the wall. The integral length scale is of the order of the pipe radius and a typical propagation speed may be taken as half the centerline velocity. This gives an estimate of the integral timescale as $2R/U_{\rm CL}$=0.03 s. For ϵ to become smaller than 1% everywhere, we find that T has to be larger than 100 s. On the other hand, if the mean velocity should only be determined at the centerline itself, the turbulence intensity is there only about 4%, and the required sampling time would be a factor hundred less!

Similar result for higher moments can also be obtained and for the second moment, i.e. $u^2_{\rm rms}$, we have

$$\epsilon^2(u^2) = 2\frac{\Lambda}{T}\left[\frac{\overline{(u^4)}}{\overline{(u^2)}^2} - 1\right] = 2\frac{\Lambda}{T}(F-1),$$

where F is the flatness factor. If u can be assumed Gaussian, then $F = 3$ and we obtain

$$\epsilon^2(u^2) = 4\frac{\Lambda}{T}.$$

The results show that to obtain $u_{\rm rms}$ with an error less than 1%, we need a sampling time longer than $40\,000\Lambda$ which in the pipe-flow experiment with air mentioned above would require 1800 s or 30 min for measurements in the viscous sublayer. For higher moments, the sampling time will be even longer to obtain the similar accuracy.

These examples clearly show that in order to obtain high accuracy results in a large facility it is of utmost importance to be able to have stationary and drift-free conditions both for the facility itself and the measurement equipment. When measurements are made at low velocities, this issue becomes even more critical since the averaging time must increase to obtain the same statistical accuracy, hence the time-averaging issue is opposite to that of the probe resolution.

7. Conclusions

Simulations of turbulence are regularly moved to the largest and most expensive computers worldwide, but are still far from replicating the high Reynolds numbers found in nature and various critical technologies. Experiments, on the other hand, are still usually made under

rather primitive conditions and using fairly small-scale facilities, typically involving only one laboratory or research group. The need for a large-scale collaborative experimental effort in order to address and resolve several critical research issues within the turbulence area is hopefully evidenced from the present paper. The fully developed turbulent pipe flow is an ideal configuration to study high Reynolds number turbulence where homogeneous conditions can be achieved experimentally with relative ease. The CICLoPE project may be a first step toward a new approach on how to carry out experimental turbulence research in the future.

Acknowledgments

We acknowledge the input from Carlo Casciola and Renzo Piva (Università di Roma 'La Sapenzia'), Martin Oberlack and Michael Frewer (TU Darmstadt), Ivan Marusic (University of Melbourne) and Timothy B Nickels (Cambridge University) who, in connection with the workshop in Bertinoro in September 2005, formulated the research issues discussed in section 4. Dr Ines Fabbro from the University of Bologna and Dr Marina Flamigni from Provincia di Forli for the invaluable work concerning the transfer of the properties of the tunnel complex and the project funding. Dr Gianluca Piraccini, Dr Maurizio Tappi, Mr Paolo Proli and Alessandro Rossetti are also thanked for their contribution during the design phase of the pipe. The KTH group thanks the Swedish foundation for international cooperation in research and higher education (STINT) for providing a grant for cooperation between KTH and the University of Bologna.

References

Abe H, Kawamura H and Matsuo Y 2004 Surface heat-flux fluctuations in a turbulent channel flow up to $Re_\tau = 1020$ with $Pr = 0.025$ and 0.71 *Int. J. Heat Fluid Flow* **25** 404–19

Andreas E L, Claffey K J, Jordan R E, Fairall C W, Guest P S, Persson P O G and Grachev A A 2006 Evaluations of the von Kármán constant in the atmospheric surface layer *J. Fluid Mech.* **559** 117–49

Christensen K T and Adrian R J 2001 Statistical evidence of hairpin vortex packets in wall turbulence *J. Fluid Mech.* **431** 433–43

Coles D E and Hirst E A 1969 Computation of turbulent boundary layers —*1968 AFOSR-IFP-Stanford Conference* vol 2 Stanford University

Q5

Davidson P A, Nickels T B and Krogstad P-A 2006 The logarithmic structure function law in wall-layer turbulence *J. Fluid Mech.* **550** 51–60

Hoyas S and Jiménez J 2006 Scaling of the velocity fluctuations in turbulent channels up to Re = 2003 *Phys. Fluids* **18** 011702

Jacob B, Biferale L, Iuso G and Casciola C M 2004 Anisotropic fluctuations in turbulent shear flows *Phys. Fluids* **16** 4135–42

Khujadze G and Oberlack M 2004 DNS and scaling laws from new symmetry groups of ZPG turbulent boundary layer flow *Theoret. Comput. Fluid Dyn.* **18** 391–411

Knobloch K and Fernholz H 2004 Statistics, correlations, and scaling in a turbulent boundary layer at $\mathrm{Re}_{\delta_2} \leqslant 1.15 \times 10^5$ *IUTAM Symp. Reynolds number scaling in turbulence, Princeton University, USA, 11–13 September* (Dordrechr: Kluwer) p 11

Kunkel G J and Marusic I 2006 Study of the near-wall-turbulent region of the high-Reynolds-number boundary layer using an atmospheric flow *J. Fluid Mech.* **548** 375–402

Laufer J 1954 The structure of turbulence in fully developed pipe flow *NACA Report* 1174

Lindgren B, Österlund J and Johansson A V 1998 Measurement and calculation of guide vane performance in expanding bends for wind-tunnels *Exp. Fluids* **24** 265–72

Lindgren B and Johansson A V 2004 Evaluation of a new wind tunnel with expanding corners *Exp. Fluids* **36** 197–203

Q5

Lindgren B, Österlund J M and Johansson A V 2004 Evaluation of scaling laws derived from Lie group symmetry methods in zero-pressure-gradient turbulent boundary layers *J. Fluid Mech.* **502** 127–52

Marati N, Casciola C M and Piva R 2004 Energy cascade and spatial fluxes in wall turbulence *J. Fluid Mech.* **521** 191–215

McKeon B J, Li J, Jiang W, Morrison J F and Smits A J 2004 Further observations on the mean velocity distribution in fully developed pipe flow *J. Fluid Mech.* **501** 135–47

Metzger M M and Klewicki J C 2001 A comparative study of near-wall turbulence in high and low Reynolds number boundary layers *Phys. Fluids* **13** 692–701

Monty J P 2005 Developments in smooth wall turbulent duct flows *PhD Thesis* Department of Mechanic and Manufacturing Engineering, University of Melbourne

Nagib H M, Chauhan K A and Monkewitz P A 2005 Scaling of high Reynolds number turbulent boundary layers revisited *AIAA paper* 2005–4810

Nagib H M, Christophorou C and Monkewitz P A 2006 High Reynolds number turbulent boundary layers subjected to various pressure-gradient conditions *'IUTAM Symposium on One Hundred Years of Boundary Layer Research: Proc. IUTAM Symposium DLR-Göttingen, Germany, 12–14 August 2004'* (Berlin: Springer) pp 383–94

Nagib H M, Chauhan K A and Monkewitz P A 2007 Approach to an asymptotic state for ZPG turbulent boundary layers *Phil. Trans. R. Soc.* A **365** 755–70

Nickels T B, Maurusic I, Hafez S and Chong M S 2005 Evidence of the k_1^{-1} law in a high-Reynolds-number turbulent boundary layer *Phys. Rev. Lett.* **95** 074501

Nikuradse J 1932 Gesetzmässigkeit der turbulenten Strömung in glatten Rohren *Forschg. Arb. Ing.–Wes.* **356**

Oberlack M 2001 A unified approach for symmetries in plane parallel turbulent shear flows *J. Fluid Mech.* **427** 299–328

Österlund J M, Lindgren B and Johansson A V 2003 Flow structures in zero pressure-gradient turbulent boundary layers at high Reynolds numbers *Eur. J. Mech.* **22** 379–90

Österlund J M, Johansson A V, Nagib H M and Hites M H 2000 A note on the overlap region in turbulent boundary layers *Phys. Fluids* **12** 1–4

Satake S, Kunugi T and Himeno R 2000 High Reynolds number computation for turbulent heat transfer in a pipe flow *High Performance Computing (Lecture Notes in Computer Science vol 1940)* (Berlin: Springer) pp 514–23

Shockling M A, Allen J J and Smits A J 2006 Roughness effects in turbulent pipe flow *J. Fluid Mech.* **564** 267–85

Sreenivasan K R, Chambers A J and Antonia R A 1978 Accuracy of moments of velocity and scalar fluctuations in the atmospheric surface layer *Bound. Layer Meteorol.* **14** 341–59

Tsuji Y, Fransson J H M, Alfredsson P H and Johansson A V 2007 Pressure statistics in high Reynolds number turbulent boundary layer *J. Fluid Mech.* **585** 1–40

van Doorne C W H and Westerweel J 2007 Measurement of laminar, transitional and turbulent pipe flow using stereoscopic-PIV *Exp. Fluids* **42** 259–79

Wygnanski I J and Champagne F H 1973 On transition in a pipe. Part 1. The origin of puffs and slugs and the flow in a turbulent slug *J. Fluid Mech.* **59** 281–335

Zagarola M V and Smits A J 1998 Mean-flow scaling of turbulent pipe flow *J. Fluid Mech.* **373** 33–79

Zanoun E-S, Durst F and Nagib H 2003 Evaluating the law of the wall in two-dimensional fully developed turbulent channel flows *Phys. Fluids* **15** 3079–89

Q5

QUERY FORM

JOURNAL: fdr

AUTHOR: A Talamelli *et al*

TITLE: CICLoPE—a response to the need for high Reynolds number experiments

ARTICLE ID: fdr303072

Page 1

Q1.
Please specify and provide the e-mail address of the corresponding author.

Q2.
Please update.

Page 6

Q3.
Please define PIV.

Page 7

Q4.
Please define MTL.

Page 20

Q5.
Please cite references Coles DE and Hirst E A 1969, Lindgren B and Johansson A V 2004 and Nagid *et al* 2005 at appropriate places in the text.